Published in final edited form as:
Curr Mol Med. 2013 December ; 13(10): 1633–1645.

Biomedical Applications of Zinc Oxide Nanomaterials

Yin Zhang[1], **Tapas R. Nayak**[2], **Hao Hong**[2], and **Weibo Cai**[1,2,3,*]

[1] Department of Medical Physics, University of Wisconsin - Madison, WI, USA

[2] Department of Radiology, University of Wisconsin - Madison, WI, USA

[3] University of Wisconsin Carbone Cancer Center, Madison, WI, USA

Abstract

Nanotechnology has witnessed tremendous advancement over the last several decades. Zinc oxide (ZnO), which can exhibit a wide variety of nanostructures, possesses unique semiconducting, optical, and piezoelectric properties hence has been investigated for a wide variety of applications. One of the most important features of ZnO nanomaterials is low toxicity and biodegradability. Zn^{2+} is an indispensable trace element for adults (~10 mg of Zn^{2+} per day is recommended) and it is involved in various aspects of metabolism. Chemically, the surface of ZnO is rich in -OH groups, which can be readily functionalized by various surface decorating molecules. In this review article, we summarized the current status of the use of ZnO nanomaterials for biomedical applications, such as biomedical imaging (which includes fluorescence, magnetic resonance, positron emission tomography, as well as dual-modality imaging), drug delivery, gene delivery, and biosensing of a wide array of molecules of interest. Research in biomedical applications of ZnO nanomaterials will continue to flourish over the next decade, and much research effort will be needed to develop biocompatible/biodegradable ZnO nanoplatforms for potential clinical translation.

Keywords

Zinc oxide; molecular imaging; cancer; nanosensor; drug delivery; gene delivery; personalized medicine

INTRODUCTION

Over the last decade, nanotechnology has been one of the fastest-growing areas of science and technology with tremendous advancement being made. The unique physicochemical properties of various nanomaterials make it possible to create new structures, systems, nanoplatforms, or devices with potential applications in a wide variety of disciplines. The development of biocompatible, biodegradable, and functionalized nanomaterials for biomedical applications has been an extremely vibrant research area. To date, the most well-studied nanomaterials for biomedical applications include quantum dots (QDs) [1, 2], carbon nanotubes (CNTs) [3, 4], nanoshells [5], paramagnetic nanoparticles [6], among many others [7-10].

Zinc oxide (ZnO), which can exhibit a wide variety of nanostructures (**Fig. (1)**), possesses unique semiconducting, optical, and piezoelectric properties [11, 12]. Therefore, ZnO-based nanomaterials have been studied for a wide variety of applications such as nano-electronic/

Weibo Cai, PhD, Departments of Radiology and Medical Physics, University of Wisconsin - Madison, 1111 Highland Ave, Room 7137, Madison, WI 53705-2275, USA. Fax: 1-608-265-0614; Tel: 1-608-262-1749; wcai@uwhealth.org..

nano-optical devices, energy storage, cosmetic products, nanosensors, etc. [13-18]. ZnO is a wide band gap semiconductor (3.37 eV) with high exciton binding energy (60 meV), which leads to efficient excitonic blue and near-UV emission [19]. The use of ZnO in sunscreens has been approved by the food and drug administration (FDA) due to its stability and inherent capability to absorb UV irradiation.

One of the most important features of ZnO nanomaterials is low toxicity and biodegradability. Zn^{2+} is an indispensable trace element for adults and it is involved in various aspects of metabolism. 11.0 mg and 9.0 mg of Zn^{2+} per day is recommended for adult men and women in the United States, respectively. Chemically, the surface of ZnO is rich in -OH groups, which can be readily functionalized by various surface decorating molecules [20, 21]. ZnO can slowly dissolve in both acidic (e.g. in the tumor cells and tumor microenvironment) and strong basic conditions if the surface is in direct contact with the solution [22]. Based on these desirable properties, ZnO nanomaterials have gained enormous interest in biomedical applications. In this review, we will summarize the current status of the use of ZnO nanomaterials for biomedical applications, such as biomedical imaging, drug delivery, gene delivery, and biosensing.

BIOIMAGING WITH ZNO NANOMATERIALS

Being inexpensive and convenient, fluorescence imaging has been widely used in preclinical research [23-26]. Since ZnO nanomaterials exhibit efficient excitonic blue and near-UV emission, which can also have green luminescence related to oxygen vacancies [27, 28], many reports exist in the literature on the use of ZnO nanomaterials for cellular imaging.

Taking advantage of their intrinsic fluorescence, the penetration of ZnO nanoparticles in human skin was imaged in vitro and in vivo [29]. It was found that most ZnO nanoparticles stayed in the stratum corneum with low possibility to result in safety concerns. In another study, biocompatible ZnO nanocrytstals (NCs) with nonlinear optical properties were synthesized, encapsulated within the nonpolar core of phospholipid micelles, and conjugated with folic acid (FA) for nonlinear optical microscopy [30]. The micelle encapsulated ZnO NCs were stable in aqueous solutions and FA-conjugated ZnO NCs were found to accumulate intracellularly throughout the cytoplasm, without inducing cytotoxicity in live KB cells which express high levels of the folate receptor. Recently, transferrin-conjugated green fluorescent ZnO NCs were also reported for cancer cell imaging with minimum cytotoxicity [31].

The optical properties of ZnO nanomaterials can be tuned by doping with appropriate elements [32]. In one report, ZnO NCs were doped with different cations (Co, Cu, or Ni) and stabilized in aqueous colloidal solutions, which were employed for cellular imaging studies in various cells [33]. It was suggested that these small ZnO nanoparticles could penetrate into the cell nucleus.

Heterostructural ZnO/Au nanocomposites, where Au NCs grow at the tip of ZnO nanorods or along the nanorod surfaces, were synthesized and investigated for their optical properties and biocompatibility [34]. It was shown that the number of Au NCs on ZnO nanorods can be controlled by changing the molar ratio of ZnO to $HAuCl_4$, with the resulting nanocomposites exhibiting tunable UV/visible emission intensity and excellent biocompatibility. When incubated with HeLa cells, these ZnO/Au nanocomposites were found to be internalized into the endosomes and cytosol. Nanoparticles of ~200 nm in diameter, where nanoscale ZnO was used to coat fluorescent dye-encapsulating SiO_2, have been reported for the imaging of E. coli [35]. In addition, these nanoparticles showed selective cytotoxicity to bacteria, as well as preferential killing of leukemic T cells while sparing normal immune cells, because of the dissolution of surface ZnO layer. In a recent

study, anti-epidermal growth factor receptor antibody-conjugated ZnO nanorods were used for imaging of cancer cells in vitro [36]. However, the emission maximum of 377 nm for these ZnO nanorods is not optimal for further investigation.

The most extensively studied nanoparticles for optical imaging are QDs due to their many desirable optical properties [1, 37, 38]. However, the commonly used CdSe or CdTe cores of QDs possess potential toxicity to biological systems. Therefore, much effort has been devoted to the development of less toxic fluorescent nanoparticles such as ZnO-based QDs. Because of the relatively weak emission and low stability of ZnO-based QDs in aqueous solutions, various strategies for surface coating have been investigated.

In one report, ZnO@polymer core-shell nanoparticles with emission in the green and yellow range and high stability in aqueous solutions were reported [39]. ZnO cores were coated with a double-layer of polymer shell (a hydrophobic inside layer and an external hydrophilic layer) to make them water soluble, as well as to improve the quantum yield. It was demonstrated that the emission wavelength of these ZnO QDs could be tuned by changing the particle size, with quantum yields of > 50%. When applied for in vitro cell imaging, the ZnO QDs were found to be located in the cytoplasm, exhibiting stable luminescence under UV light without significant cytotoxicity. In a follow-up study, similar QDs were tested in mice after intradermal and intravenous injections [40]. It was found that the fluorescence signal from QDs could be detected for > 90 minutes after intradermal injection. However, the QD fluorescence could only be observed within 30 minutes after intravenous injection, mostly in the vessels, liver, and kidneys. Toxicity study after intravenous injection demonstrated that the ZnO QDs did not show any acute toxicity to mice within 24 hours. For future studies, more stable surface coating will be needed for these ZnO QDs and longer circulation half-life will also be more favorable.

Each of the imaging techniques has its own advantages as well as disadvantages [41]. Nanomaterials can be functionalized to be detectable by multiple imaging modalities, which can provide synergistic advantages [2, 10]. When compared with small molecules, nanomaterials are more suitable for multimodality imaging because of the large surface area which provides more sites for functionalization, as well as the possibility to engineer them for multimodal detection. In one interesting study, Gd-doped ZnO QDs (with sizes of < 6 nm) were developed for both optical and magnetic resonance imaging (MRI) (**Fig. (2)**) [42]. It was found that the emission intensity of the Gd-doped ZnO QDs increased with increasing concentration of Gd^{3+}, with maximum emission intensity at 550 nm. Upon surface coating with N-(2-aminoethyl) aminopropyltrimethoxysilane (AEAPS), the resulting Gd-doped ZnO QDs exhibited low toxicity to HeLa cells and could be imaged with both confocal microscopy and MRI in vitro. In another study, multifunctional Fe_3O_4-ZnO core-shell magnetic QDs were also reported for potential cancer imaging and therapy [43].

The major hurdles for biomedical applications of ZnO nanomaterials include low-intensity and short-wavelength luminescence of ZnO, limited capability in size control, and sharpness/stiffness of ceramic-based nanostructures (rigid and sharp tips/edges could potentially cause cell/tissue damage). We recently synthesized green fluorescent ZnO nanowires (NWs), which could overcome the abovementioned hurdles, and demonstrated that the ZnO NWs can be employed for targeted imaging of cancer cells [44, 45]. The c(RGDyK) (abbreviated as RGD) peptide, which is a potent antagonist of integrin $\alpha_v\beta_3$ (a key protein involved in tumor angiogenesis and metastasis) [46, 47], was used as the targeting ligand. After surface functionalization to render the ZnO NWs water solubility, better biocompatibility, and lower cytotoxicity, RGD-conjugated green fluorescent ZnO NWs selectively bound to U87MG human glioblastoma cells (which express a high level of

integrin $\alpha_v\beta_3$) and the intrinsic fluorescence signal of ZnO NWs could be detected by a fluorescence microscope (**Fig. (3A,B)**).

In addition, these ZnO NWs were also labeled with a positron emission tomography (PET) isotope, ^{64}Cu ($t_{1/2}$: 12.7 h), to evaluate its biodistribution in normal mice without the use of tumor-targeting ligands (e.g. RGD peptides) [44]. PET findings revealed that the ZnO NWs accumulated mainly in the reticuloendothelial system (RES) and they could be degraded and cleared from the mouse body (**Fig. (3C)**). Much further improvement will be needed before these ZnO NWs can be applied for in vivo targeting/imaging of cancer. For example, the size of ZnO NWs can be reduced to improve the tumor targeting efficiency; ZnO NWs with fluorescence emission in the red or near-infrared (NIR) region are preferred which will have better tissue penetration of the optical signal; the in vitro/in vivo stability of the ZnO NWs needs to be evaluated and the long term toxicity should be studied. Since the major obstacle facing most nanomaterial-based tumor targeting is efficient extravasation [10, 48], by targeting integrin $\alpha_v\beta_3$ which is overexpressed on both tumor vasculature and certain tumor cells, RGD-conjugated ZnO nanomaterials could have desirable in vivo tumor targeting efficiency because extravasation is not needed for active tumor targeting.

To date, the use of radiolabeled, molecularly targeted ZnO nanomaterials has not been reported yet. Radionuclide-based imaging techniques (i.e. PET [49-55] and single-photon emission computed tomography [SPECT] [56-60]) have much better clinical relevance, hence are more widely used in the clinic than optical imaging. Not only is there no tissue penetration limit for these techniques, PET and SPECT are also highly quantitative and sensitive [41, 49, 61-64]. Therefore, PET and SPECT only require tracer concentration many orders of magnitude lower than the pharmacologically active level, which will have little biological adverse effects. Combination of the high sensitivity of PET and intrinsic fluorescence of ZnO nanomaterials through the use of radiolabeled ZnO nanomaterials can provide synergistic advantages and greatly facilitate the development of ZnO nanomaterial-based anti-cancer agents and their future clinical translation. PET, which detects the radiolabel rather than ZnO itself, is sensitive, quantitative, and clinically relevant. Optical imaging can provide inexpensive and convenient tracking of the ZnO nanomaterial itself in animal models. Further, the intrinsic fluorescence of ZnO nanomaterials can enable microscopy/histology studies without exogenous dyes, which can serve as a convenient and robust means for validation of the in vivo findings in animal models.

DRUG DELIVERY WITH ZNO NANOMATERIALS

ZnO nanomaterials are versatile nanoplatforms for not only bioimaging but also drug delivery applications, due to their large surface area, versatile surface chemistry, phototoxic effect, among others. In vitro studies have shown that ZnO nanoparticles can be highly toxic to cancer cells [65] or bacteria and leukemic T cells [35]. Therefore, not only have ZnO nanomaterials been investigated as drug/gene delivery vehicles, they have also been studied for cancer therapy.

ZnO QDs with intrinsic blue fluorescence were coated with folate-conjugated chitosan via electrostatic interaction, which could be loaded with doxorubicin (DOX, a widely used chemotherapy drug) at ~75% efficiency [66]. It was suggested that DOX was entrapped through interaction with the surface of ZnO QDs and/or folate via hydrogen bonding, whereas the external chitosan layer enhanced aqueous stability of the ZnO QDs due to the charges and hydrophilicity. However, DOX was released quickly at the normal physiological pH value of 7.4, which needs to be improved for future in vitro/in vivo studies.

One of the major obstacles in dendritic cell (DC)-based cancer immunotherapy is the development of a delivery system which can efficiently deliver target antigens into DCs [67]. Because of the large surface area, nanomaterials are promising candidates for this application. Recently, Fe_3O_4-ZnO core-shell nanoparticles with an average diameter of 16 nm were prepared to deliver carcinoembryonic antigen into DCs, which could also serve as imaging contrast agents (**Fig. (4)**) [68]. Antigen-bound nanoparticles were efficiently taken up by DCs in vitro, where the ZnO shell facilitated cell internalization and significantly reduced the incubation time needed for labeling DCs. No changes in viability or phenotype were observed in the nanoparticle-labeled DCs. More importantly, the uptake of nanoparticle-labeled DCs in draining lymph nodes of a mouse was successfully detected by MRI, warranting future investigation of these nanoparticles for image-guided antigen delivery and in vivo tracking of the loaded DCs.

The cytotoxicity of aminopolysiloxane capped ZnO nanoparticles of different sizes (20, 60, and 100 nm, respectively) was evaluated in leukemia K562 and adriamycin-resistant K562/A02 cells [69]. The K562/A02 cells were found to be more sensitive to ZnO nanoparticles than K562 cells. Furthermore, ZnO nanoparticles of different sizes showed different cytotoxic effects on the two cell lines, where cell proliferation could be suppressed by UV irradiation after incubation with ZnO nanoparticles. The synergistic cytotoxic effect of the three ZnO nanoparticles and daunorubicin (DNR; which can cause DNA damage and induce apoptosis in cells) against leukemia cells was also explored, and the presence of ZnO nanoparticles were shown to enhance cellular uptake of DNR and inhibit proliferation of the two cell lines. In a subsequent study, similar results were achieved in hepatocellular carcinoma SMMC-7721 cells [70].

Photodynamic therapy (PDT) is an emerging and promising alternative for non-invasive treatment of cancer [71]. Upon uptake of photosensitizers into cancer cells, irradiation with light of suitable wavelength and dosage can generate reactive oxygen species (ROS) which can induce cell death and/or necrosis [72]. ZnO nanoparticles can induce ROS such as hydroxyl radical, hydrogen peroxide, and superoxide in aqueous solutions upon absorption of UV illumination, making them good candidates for PDT (**Fig. (5)**) [73]. For cancer therapy, combination of different regimens can often lead to better efficacy, reduce side effects, and decrease the likelihood of drug resistance. In a proof-of-concept study, ZnO nanorods of sizes 20 nm × 50 nm which exhibited minimal cellular cytotoxicity by themselves were used to deliver DNR for combination therapy in SMMC-7721 cells (**Fig. (6)**) [73]. Due to the negative surface charges of ZnO nanorods, positively charged DNR self-assembled onto the nanorods via electrostatic interaction. The binding between DNR and ZnO nanorods was found to be pH sensitive and DNR could be released gradually with decreasing pH (**Fig. (6B)**), which is desirable since tumor microenvironment is typically acidic. Cellular uptake of DNR was significantly increased when it is attached to ZnO nanorods and enhanced anti-cancer efficacy of DNR-loaded ZnO nanorods was achieved. UV illumination could further induce apoptosis of SMMC-7721 cells by photocatalysis of ZnO nanorods (**Fig. (6C,D)**).

GENE DELIVERY WITH ZNO NANOMATERIALS

Gene therapy has attracted considerable interest over the last several decades for cancer treatment [74]. One major challenge of gene therapy is the development of safe gene vectors which can protect DNA from degradation and enable cellular uptake of DNA with high efficiency. A wide variety of nanomaterials have been investigated for gene delivery and gene therapy applications, including ZnO nanomaterials which have shown promise in various literature reports.

In a series of studies, three-dimensional tetrapod-like ZnO nanostructures were investigated as gene vectors to deliver pEGFPN1 DNA (which contains the gene for green fluorescent protein) to A375 human melanoma cells [75, 76]. The plasmid DNA (pDNA) was attached to ZnO nanostructures via electrostatic interactions, and the three needle-shaped legs favored the internalization of the tips within the cells for gene delivery. No significant cytotoxicity was observed, which was reportedly attributed to the three dimensional geometry.

Surface-coating of nanomaterials plays a critical role in efficient gene delivery. In one report, ZnO QDs coated with positively charged poly(2-(dimethylamino)ethyl methacrylate) (PDMAEMA) polymers were used to condense pDNA for gene delivery [77]. The polymer-coated ZnO QDs exhibited fluorescence emission at 570 nm with quantum yield of >20%, which was able to condense large pDNA such as a luciferase reporter gene. It was demonstrated that COS-7 cells could be efficiently transfected with pDNA-carrying ZnO QDs with low cytotoxicity. When compared with the use of PDMAEMA itself as the gene vector, the ZnO QDs had significantly reduced cytotoxicity due to the presence of negative charged polymethacrylate in the QDs which counteracted the positive charges.

BIOSENSORS BASED ON ZNO NANOMATERIALS

Biosensors (e.g. photometric, calorimetric, electrochemical, piezoelectric, among others when categorized based on the detection principles) are widely used in healthcare, chemical/biological analysis, environmental monitoring, and food industry [78]. Nanomaterials, alone or in combination with biologically active substances, are attracting ever-increasing attention since they can provide a suitable platform for the development of high performance biosensors due to their unique properties [17]. For example, the high surface area of nanomaterials can be employed to immobilize various biomolecules such as enzymes, antibodies, and other proteins. In addition, they can allow for direct electron transfer between active sites of the biomolecules and the electrode.

Besides semiconducting properties, ZnO nanomaterials also exhibit various desirable traits for biosensing such as high catalytic efficiency, strong adsorption capability, and high isoelectric point (IEP; ~9.5) which are suitable for adsorption of certain proteins (e.g. enzymes and antibodies with low IEPs) by electrostatic interaction [79]. Furthermore, high surface area, good biocompatibility/stability, low toxicity, and high electron transfer capability also make them promising nanomaterials for biosensors [80]. The majority of reported ZnO-based biosensors are for the detection of various small molecule analytes such as glucose, phenol, H_2O_2, cholesterol, urea, etc. (**Table 1**). In addition, there are also various biosensors for other molecules of interest and certain chemical/physical properties such as pH [81, 82]. Interested readers are referred to several excellent review articles on this topic for more detailed discussion [17, 78, 83]. Herein we will give a brief overview of this area and only discuss selected literature reports.

Glucose Biosensors

Glucose biosensors, using glucose oxidase (GOx) as the enzyme, can be used both in the clinic (e.g. for diagnosis of diabetes) and in food industry. Early stage ZnO-based biosensors were fabricated by loading GOx onto single crystal ZnO nanocombs [79], NWs [84], or NW arrays [85] by physical adsorption, which exhibited high sensitivity because of the strong affinity of GOx to glucose. Other biosensors have been constructed by immobilizing GOx electrostatically onto a supporting matrix made up of ZnO nanorods [86] or crystallized ZnO nanonails [87], which had good stability, high sensitivity, and short response time (e.g. 10s) for glucose detection due to direct electron transfer between the active sites of immobilized GOx and the electrode surface. A variety of other GOx-based glucose biosensors have also

been reported using tetragonal pyramid-shaped porous ZnO nanostructures fabricated on a glassy carbon electrode (GCE) [88], ZnO nanorod/Au nanocrystal matrix [89], ZnO nanoclusters doped with Co [90], carbon-decorated ZnO NW array [91], and vertically grown ZnO NW coated with a monolayer of ZnS NCs [92].

Recently, several interesting reports appeared on ZnO-based glucose biosensors. In one study, multiwalled CNTs on the GCE was used to immobilize the first layer of GOx and electrodeposited ZnO nanoparticles were coated with a second layer of GOx [93]. Rapid response to glucose with a detection limit of 2.22 □M was achieved with this biosensor. Another approach was based upon the variation in fluorescence signal of ZnO NCs with different glucose concentrations [94]. The ZnO NCs were covalently functionalized with GOx, which gave a fast response time of 5s and a lower detection limit of 0.33 mM.

Phenol Biosensors

Phenolic compounds are highly toxic to animal and plants. Since they commonly exist in industrial waste, it is important to detect and measure them for environmental monitoring. Among the many analytical methods developed for detection of phenolic compounds, biosensors based on immobilization of tyrosinase were shown to be convenient, high sensitive, and effective [95, 96]. Many of these biosensors have been fabricated on a platform of ZnO nanoparticles, because of the inherent electrostatic attraction between electropositive ZnO nanostructures and tyrosinase, which has a low IEP of 4.6 [97].

Tyrosinase has been adsorbed onto different ZnO nanomaterials such as ZnO sol-gel matrix [98], ZnO nanoparticles [99], and ZnO nanorods [100] through electrostatic interaction, which were further immobilized on a GCE. Similarly, a biosensor was constructed by immobilizing tyrosinase onto ZnO nanorod clusters supported by nanocrystalline diamond electrodes [101]. These abovementioned ZnO nanomaterials not only provided strategic microenvironment for tyrosinase loading due to its favourable IEP but also helped in retaining the enzymatic activity, which enabled sensitive detection of phenolic compounds.

To improve biosensor performance, ZnO nanostructures were fabricated on gold wires to facilitate the nucleation for growth, which resulted in a response time of <5s [102]. Recently, a biosensor based on ZnO nanorod microarrays on boron-doped nanocrystalline diamond substrates was reported [103]. Since tyrosinase was covalently immobilized to ZnO nanorods, this sensor showed very high sensitivity for p-cresol, 4-chlorophenol, and phenol (576.2, 339.3, and 287.1 □A cm^{-2} mM^{-1} respectively). In another biosensor design, tyrosinase was encapsulated by CNT-ZnO-nafion composite film on GCE, which exhibited excellent sensitivity and a very fast response time of 2s [104].

H_2O_2 Biosensors

Recently, detection of H_2O_2 has become a vibrant research area as it plays an important role in the food industry, environmental monitoring, and clinical diagnosis [105]. For H_2O_2 detection, the enzyme horse radish peroxidase (HRP) is commonly used due to its high selectivity. In one report, ZnO in the form of nanosized flowers, dispersed in chitosan solution to form ZnO/chitosan composite matrix which was further immobilized with HRP, were used to generate a biosensor with good reproducibility and stability [106]. Another H_2O_2 biosensor was constituted by co-immobilizing waxberry-like ZnO microstructure composed of 8-10 nm nanorods with HRP onto the surface of a GCE [107]. A biosensor based on ZnO nanorods fabricated on gold wire, with multilayer immobilization of HRP, was also reported [108]. The multiple layers of HRP not only enhanced the detection sensitivity, due to better affinity effect of HRP to the catalysed target, but also decreased the response time considerably to ~5s.

Cholesterol Biosensors

Cholesterol is an important molecule for humans and serum cholesterol level is an indicator for various diseases such as hypertension, myocardial infarction, and arteriosclerosis [109, 110]. Therefore, many biosensors have been developed for fast measurement of cholesterol concentration [111]. These biosensors were constructed by immobilizing cholesterol oxidase, through either physical absorption or electrostatic interaction, onto various ZnO nanomaterials such as ZnO nanoporous thin films grown on gold surface [112], well-crystallized flower-shaped ZnO structures [113], electrodeposited ZnO nanospheres incorporated with Pt onto a GCE [114], gold/platinum hybrid functionalized ZnO nanorods constructed on multiwalled CNT modified GCE [115], hexagon-shaped ZnO nanorods grown on silver wire [116], or ZnO nanowalls chemically fashioned on aluminium wires [117].

Urea Biosensors

Urea plays a critical role in the metabolism of nitrogen-containing compounds in the human body. Abnormal urea levels in the blood and urine may lead to renal failure, urinary tract obstruction, dehydration, shock, gastrointestinal bleeding, etc. Therefore, measurement of urea in the blood and serum is important for the diagnosis of renal and liver diseases. In urea biosensors, the enzyme urease is generally used to catalyse the conversion of urea into hydrogen carbonate and ammonium [118].

The first urea biosensor based on ZnO nanomaterials was reported in 2008, in which urease was immobilized onto ZnO-chitosan nanobiocomposite film on indium-tin-oxide coated glass by physical adsorption [119]. Subsequently, a similar biosensor was fabricated using the same design but without chitosan, which gave significantly lower detection sensitivity [120]. Another biosensor based on amperometric detection of urea was constructed by electrostatically immobilizing urease to ZnO nanorods grown onto indium-tin-oxide coated glass, which had a response time of 3s and a detection limit of 0.13 mM urea [121]. Recently, ZnO NW arrays fabricated on gold coated plastics were also utilized in a urea biosensor, where urease was immobilized by physical adsorption [122].

Other Biosensors

Aside from the biosensors mentioned above, many other biosensors have been reported for the detection of a wide variety of molecules. For example, films of ZnO nanoparticles and NWs impregnated with 1% Pt or doped with Mn and Co have been investigated for sensing of H_2, CO, and ethanol vapour [123], showing stability over 1000 cycles. ZnO-based biosensors have also been reported for the detection of substances such as uric acid [124, 125], lactic acid [126], DNA [127, 128], proteins [129], a breast cancer marker (carbohydrate antigen 15.3) [130], among many others [17, 78].

CONCLUSION AND FUTURE PERSPECTIVES

Nanotechnology has had a revolutionary impact on biomedicine and witnessed tremendous advancement over the last several decades. With sizes less than a few hundred nm, several orders of magnitude smaller than human cells, nanomaterials can exhibit properties distinct from both molecules and bulk solids and offer unprecedented interactions with biomolecules both on the surface of and inside cells [131, 132]. With many attractive physicochemical properties and tremendous potential for various biomedical applications, ZnO nanomaterials are excellent candidates as biocompatible, biodegradable, “deliver and dissolve” nanoplatforms for cancer targeted imaging and therapy. Even though this research area is still nascent, various ZnO nanomaterials have already been evaluated for optical imaging and MRI in cells, as well as dual-modality MRI/optical imaging. For in vivo imaging and

therapy applications, the future of nanomedicine lies in multifunctional nanoplatforms combining both therapeutic components and multimodality imaging, so that the therapeutic efficacy could be not only improved but also accurately monitored non-invasively over time. To date, no in vivo targeted imaging with ZnO nanomaterials has been reported, which deserves significant research effort in the near future.

For applications of nanomaterials in biomedicine, the biocompatibility is always a concern. Even though ZnO has been approved for cosmetic uses by the FDA, the detailed toxicological profile and the mechanism of cytotoxicity for ZnO nanomaterials is not yet well elucidated [133]. Many studies have focused on the biocompatibility of ZnO nanomaterials without surface coating/modifications. For example, it was reported that ZnO nanoparticles showed cytotoxic effect above certain concentrations and the toxicity was pH dependent, due to the increased concentration of Zn^{2+} in the culture medium or inside cells from dissolved ZnO [134]. Nonetheless, such leakage of ionic Zn^{2+} into the biological system from dissolution of ZnO can perhaps be well-tolerated since ~10 mg/day of Zn^{2+} is needed for adults. Meanwhile, other reports have shown that ZnO nanomaterials were nontoxic and preferentially toxic to bacteria or cancer cells [35, 65], which could be advantageous for cancer therapy applications.

Surface modification of nanomaterials plays a crucial role for potential biomedical applications. It has been demonstrated that the biocompatibility of ZnO nanomaterials could be improved by slowing down the dissolution rate through Fe doping [135] or surface capping [136]. We believe that the key question to ask is not how toxic “naked” ZnO nanomaterials are, but how to functionalize/modify them so that they exhibit minimum potential toxicity, can be cleared from the human body, and thus can be applied in biological systems. To date, most of the reported toxicology studies of ZnO nanomaterials were carried out in vitro. Much effort is needed for long term in vivo toxicology studies to pave the way for future biomedical applications of these intriguing nanomaterials.

Facile conjugation of various biocompatible polymers, imaging labels, and drugs to ZnO nanomaterials can be achieved because of the versatile surface chemistry. For future biomedical applications of ZnO nanomaterials, several directions are of great importance and deserve significant research effort: 1) Labeling ZnO nanomaterials with radionuclides for PET/SPECT imaging and the use of ZnO nanomaterials for in vivo tumor targeting; 2) Development of a biocompatible/biodegradable ZnO nanomaterial platform for tumor targeted drug/gene delivery; 3) In vivo targeted PDT with drug/gene-loaded ZnO nanomaterials for combination therapy of cancer; 4) The use of dual-modality PET/optical or PET/MRI imaging, which takes advantage of the quantitation capability of PET and the intrinsic fluorescence signal of ZnO (and/or high resolution of MRI) to track ZnO nanomaterials in vivo; 5) Thorough investigation of the pharmacokinetics and long term toxicity of ZnO nanomaterials with different surface modifications; among others. Furthermore, ZnO-based biosensors and in vivo imaging are both critical for future patient management, which can provide complementary information and offer synergistic advantages. It is expected that research in biomedical applications of ZnO nanomaterials will continue to flourish over the next decade, and we hope that this timely review which gives a snapshot of this vibrant research area can attract new talents to this vibrant area.

Acknowledgments

This work is supported, in part, by the University of Wisconsin - Madison, the National Institutes of Health (NIBIB/NCI 1R01CA169365), the Department of Defense (W81XWH-11-1-0644), and the American Cancer Society (RSG-13-099-01-CCE).

REFERENCES

1. Cai W, Hsu AR, Li ZB, Chen X. Are quantum dots ready for in vivo imaging in human subjects? Nanoscale Res Lett. 2007; 2:265–81. [PubMed: 21394238]
2. Cai W, Hong H. In a “nutshell”: intrinsically radio-labeled quantum dots. Am J Nucl Med Mol Imaging. 2012; 2:136–40. [PubMed: 23133808]
3. Lacerda L, Bianco A, Prato M, Kostarelos K. Carbon nanotubes as nanomedicines: from toxicology to pharmacology. Adv Drug Deliv Rev. 2006; 58:1460–70. [PubMed: 17113677]
4. Hong H, Gao T, Cai W. Molecular imaging with single-walled carbon nanotubes. Nano Today. 2009; 4:252–61. [PubMed: 21754949]
5. Hirsch LR, Gobin AM, Lowery AR, et al. Metal nanoshells. Ann Biomed Eng. 2006; 34:15–22. [PubMed: 16528617]
6. Thorek DL, Chen AK, Czupryna J, Tsourkas A. Superparamagnetic iron oxide nanoparticle probes for molecular imaging. Ann Biomed Eng. 2006; 34:23–38. [PubMed: 16496086]
7. Cai W, Chen X. Nanoplatforms for targeted molecular imaging in living subjects. Small. 2007; 3:1840–54. [PubMed: 17943716]
8. Zhang Y, Hong H, Myklejord DV, Cai W. Molecular imaging with SERS-active nanoparticles. Small. 2011; 7:3261–9. [PubMed: 21932216]
9. Yigit MV, Medarova Z. In vivo and ex vivo applications of gold nanoparticles for biomedical SERS imaging. Am J Nucl Med Mol Imaging. 2012; 2:232–41. [PubMed: 23133814]
10. Hong H, Zhang Y, Sun J, Cai W. Molecular imaging and therapy of cancer with radiolabeled nanoparticles. Nano Today. 2009; 4:399–413. [PubMed: 20161038]
11. Wang ZL. Splendid one-dimensional nanostructures of zinc oxide: a new nanomaterial family for nanotechnology. ACS Nano. 2008; 2:1987–92. [PubMed: 19206442]
12. Yang P, Yan R, Fardy M. Semiconductor nanowire: what's next? Nano Lett. 2010; 10:1529–36. [PubMed: 20394412]
13. Huang MH, Wu Y, Feick H, et al. Catalytic Growth of Zinc Oxide Nanowires by Vapor Transport. Adv Mater. 2001; 13:113–6.
14. Fan Z, Lu JG. Zinc oxide nanostructures: synthesis and properties. J Nanosci Nanotechnol. 2005; 5:1561–73. [PubMed: 16245516]
15. Wang X, Liu J, Song J, Wang ZL. Integrated nanogenerators in biofluid. Nano Lett. 2007; 7:2475–9. [PubMed: 17604406]
16. Lao CS, Park MC, Kuang Q, et al. Giant enhancement in UV response of ZnO nanobelts by polymer surface-functionalization. J Am Chem Soc. 2007; 129:12096–7. [PubMed: 17880088]
17. Yakimova R, Selegard L, Khranovskyy V, et al. ZnO materials and surface tailoring for biosensing. Front Biosci (Elite Ed). 2012; 4:254–78. [PubMed: 22201869]
18. Yang Y, Guo W, Zhang Y, et al. Piezotronic effect on the output voltage of P3HT/ZnO micro/nanowire heterojunction solar cells. Nano Lett. 2011; 11:4812–7. [PubMed: 21961812]
19. Ozgur U, Alivov YI, Liu C, et al. A comprehensive review of ZnO materials and devices. J Appl Phys. 2005; 98:041301–103.
20. Liu D, Wu W, Qiu Y, et al. Surface functionalization of ZnO nanotetrapods with photoactive and electroactive organic monolayers. Langmuir. 2008; 24:5052–9. [PubMed: 18370437]
21. Taratula O, Galoppini E, Wang D, et al. Binding studies of molecular linkers to ZnO and MgZnO nanotip films. J Phys Chem B. 2006; 110:6506–15. [PubMed: 16570948]
22. Zhou J, Xu NS, Wang ZL. Dissolving Behavior and Stability of ZnO Wires in Biofluids: A Study on Biodegradability and Biocompatibility of ZnO Nanostructures. Adv Mater. 2006; 18:2432–5.
23. Huang X, Lee S, Chen X. Design of “smart” probes for optical imaging of apoptosis. Am J Nucl Med Mol Imaging. 2011; 1:3–17. [PubMed: 22514789]
24. Cai W, Zhang Y, Kamp TJ. Imaging of induced pluripotent stem cells: from cellular reprogramming to transplantation. Am J Nucl Med Mol Imaging. 2011; 1:18–28. [PubMed: 21841970]
25. Thorek DLJ, Robertson R, Bacchus WA, et al. Cerenkov imaging - a new modality for molecular imaging. Am J Nucl Med Mol Imaging. 2012; 2:163–73. [PubMed: 23133811]

26. Wang RE, Niu Y, Wu H, Amin MN, Cai J. Development of NGR peptide-based agents for tumor imaging. Am J Nucl Med Mol Imaging. 2011; 1:36–46. [PubMed: 23133793]
27. Heo YW, Norton DP, Pearton SJ. Origin of green luminescence in ZnO thin film grown by molecular-beam epitaxy. J Appl Phys. 2005; 98:073502–6.
28. Vanheusden K, Warren WL, Seager CH, et al. Mechanisms behind green photoluminescence in ZnO phosphor powders. J Appl Phys. 1996; 79:7983–90.
29. Zvyagin AV, Zhao X, Gierden A, et al. Imaging of zinc oxide nanoparticle penetration in human skin in vitro and in vivo. J Biomed Opt. 2008; 13:064031. [PubMed: 19123677]
30. Kachynski AV, Kuzmin AN, Nyk M, Roy I, Prasad PN. Zinc Oxide Nanocrystals for Non-resonant Nonlinear Optical Microscopy in Biology and Medicine. J Phys Chem C Nanomater Interfaces. 2008; 112:10721–4. [PubMed: 19633706]
31. Sudhagar S, Sathya S, Pandian K, Lakshmi BS. Targeting and sensing cancer cells with ZnO nanoprobes in vitro. Biotechnol Lett. 2011; 33:1891–6. [PubMed: 21553287]
32. Xue F, Liang J, Han H. Synthesis and spectroscopic characterization of water-soluble Mn-doped ZnO(x)S(1-x) quantum dots. Spectrochim Acta A Mol Biomol Spectrosc. 2011; 83:348–52. [PubMed: 21930422]
33. Wu YL, Fu S, Tok AI, et al. A dual-colored bio-marker made of doped ZnO nanocrystals. Nanotechnology. 2008; 19:345605. [PubMed: 21730654]
34. Zhang W-Q, Lu Y, Zhang T-K, et al. Controlled Synthesis and Biocompatibility of Water-Soluble ZnO Nanorods/Au Nanocomposites with Tunable UV and Visible Emission Intensity. J Phys Chem C. 2008; 112:19872–7.
35. Wang H, Wingett D, Engelhard MH, et al. Fluorescent dye encapsulated ZnO particles with cell-specific toxicity for potential use in biomedical applications. J Mater Sci Mater Med. 2009; 20:11–22. [PubMed: 18651111]
36. Yang SC, Shen YC, Lu TC, Yang TL, Huang JJ. Tumor detection strategy using ZnO light-emitting nanoprobes. Nanotechnology. 2012; 23:055202. [PubMed: 22238275]
37. Michalet X, Pinaud FF, Bentolila LA, et al. Quantum dots for live cells, in vivo imaging, and diagnostics. Science. 2005; 307:538–44. [PubMed: 15681376]
38. Medintz IL, Uyeda HT, Goldman ER, Mattoussi H. Quantum dot bioconjugates for imaging, labelling and sensing. Nat Mater. 2005; 4:435–46. [PubMed: 15928695]
39. Xiong HM, Xu Y, Ren QG, Xia YY. Stable aqueous ZnO@polymer core-shell nanoparticles with tunable photoluminescence and their application in cell imaging. J Am Chem Soc. 2008; 130:7522–3. [PubMed: 18498161]
40. Pan ZY, Liang J, Zheng ZZ, Wang HH, Xiong HM. The application of ZnO luminescent nanoparticles in labeling mice. Contrast Media Mol Imaging. 2011; 6:328–30. [PubMed: 21861292]
41. Massoud TF, Gambhir SS. Molecular imaging in living subjects: seeing fundamental biological processes in a new light. Genes Dev. 2003; 17:545–80. [PubMed: 12629038]
42. Liu Y, Ai K, Yuan Q, Lu L. Fluorescence-enhanced gadolinium-doped zinc oxide quantum dots for magnetic resonance and fluorescence imaging. Biomaterials. 2011; 32:1185–92. [PubMed: 21055806]
43. Singh SP. Multifunctional magnetic quantum dots for cancer theranostics. J Biomed Nanotechnol. 2011; 7:95–7. [PubMed: 21485821]
44. Hong H, Shi J, Yang Y, et al. Cancer-targeted optical imaging with fluorescent zinc oxide nanowires. Nano Lett. 2011; 11:3744–50. [PubMed: 21823599]
45. Shi J, Hong H, Ding Y, et al. Evolution of Zinc Oxide Nanostructures through Kinetics Control. J Mater Chem. 2011; 21:9000–8. [PubMed: 21743779]
46. Cai W, Chen X. Anti-angiogenic cancer therapy based on integrin a_vb_3 antagonism. Anti-Cancer Agents Med Chem. 2006; 6:407–28.
47. Cai W, Niu G, Chen X. Imaging of integrins as biomarkers for tumor angiogenesis. Curr Pharm Des. 2008; 14:2943–73. [PubMed: 18991712]
48. Ruoslahti E, Bhatia SN, Sailor MJ. Targeting of drugs and nanoparticles to tumors. J Cell Biol. 2010; 188:759–68. [PubMed: 20231381]

49. Gambhir SS. Molecular imaging of cancer with positron emission tomography. Nat Rev Cancer. 2002; 2:683–93. [PubMed: 12209157]
50. Alauddin MM. Positron emission tomography (PET) imaging with ^{18}F-based radiotracers. Am J Nucl Med Mol Imaging. 2012; 2:55–76. [PubMed: 23133802]
51. Cai W, Hong H. Peptoid and positron emission tomography: an appealing combination. Am J Nucl Med Mol Imaging. 2011; 1:76–9. [PubMed: 22022661]
52. Eary JF, Hawkins DS, Rodler ET, Conrad EUI. ^{18}F-FDG PET in sarcoma treatment response imaging. Am J Nucl Med Mol Imaging. 2011; 1:47–53. [PubMed: 23133794]
53. Grassi I, Nanni C, Allegri V, et al. The clinical use of PET with ^{11}C-acetate. Am J Nucl Med Mol Imaging. 2012; 2:33–47. [PubMed: 23133801]
54. Iagaru A. ^{18}F-FDG PET/CT: timing for evaluation of response to therapy remains a clinical challenge. Am J Nucl Med Mol Imaging. 2011; 1:63–4. [PubMed: 23133796]
55. Vach W, Høilund-Carlsen PF, Fischer BM, Gerke O, Weber W. How to study optimal timing of PET/CT for monitoring of cancer treatment. Am J Nucl Med Mol Imaging. 2011; 1:54–62. [PubMed: 23133795]
56. Aparici CM, Carlson D, Nguyen N, Hawkins RA, Seo Y. Combined SPECT and Multidetector CT for Prostate Cancer Evaluations. Am J Nucl Med Mol Imaging. 2012; 2:48–54. [PubMed: 22267999]
57. Bhargava P, He G, Samarghandi A, Delpassand ES. Pictorial review of SPECT/CT imaging applications in clinical nuclear medicine. Am J Nucl Med Mol Imaging. 2012; 2:221–31. [PubMed: 23133813]
58. Ogasawara Y, Ogasawara K, Suzuki T, et al. Preoperative ^{123}I-iomazenil SPECT imaging predicts cerebral hyperperfusion following endarterectomy for unilateral cervical internal carotid artery stenosis. Am J Nucl Med Mol Imaging. 2012; 2:77–87. [PubMed: 23133803]
59. Zeman MN, Scott PJH. Current imaging strategies in rheumatoid arthritis. Am J Nucl Med Mol Imaging. 2012; 2:174–220. [PubMed: 23133812]
60. Zhao R, Wang J, Deng J, Yang W, Wang J. Efficacy of ^{99m}Tc-EDDA/HYNIC-TOC SPECT/CT scintigraphy in Graves' ophthalmopathy. Am J Nucl Med Mol Imaging. 2012; 2:242–7. [PubMed: 23133815]
61. Zhang Y, Nayak TR, Hong H, Cai W. Graphene: a versatile nanoplatform for biomedical applications. Nanoscale. 2012; 4:3833–42. [PubMed: 22653227]
62. Buckle T, van den Berg NS, Kuil J, et al. Non-invasive longitudinal imaging of tumor progression using an ^{111}indium labeled CXCR4 peptide antagonist. Am J Nucl Med Mol Imaging. 2012; 2:99–109. [PubMed: 23133805]
63. De Saint-Hubert M, Brepoels L, Devos E, et al. Molecular imaging of therapy response with ^{18}F-FLT and ^{18}F-FDG following cyclophosphamide and mTOR inhibition. Am J Nucl Med Mol Imaging. 2012; 2:110–21. [PubMed: 23133806]
64. Sun M, Hoffman D, Sundaresan G, et al. Synthesis and characterization of intrinsically radio-labeled quantum dots for bimodal detection. Am J Nucl Med Mol Imaging. 2012; 2:122–35. [PubMed: 23133807]
65. Hanley C, Layne J, Punnoose A, et al. Preferential killing of cancer cells and activated human T cells using ZnO nanoparticles. Nanotechnology. 2008; 19:295103. [PubMed: 18836572]
66. Yuan Q, Hein S, Misra RD. New generation of chitosan-encapsulated ZnO quantum dots loaded with drug: synthesis, characterization and in vitro drug delivery response. Acta Biomater. 2010; 6:2732–9. [PubMed: 20100604]
67. Figdor CG, de Vries IJ, Lesterhuis WJ, Melief CJ. Dendritic cell immunotherapy: mapping the way. Nat Med. 2004; 10:475–80. [PubMed: 15122249]
68. Cho NH, Cheong TC, Min JH, et al. A multifunctional core-shell nanoparticle for dendritic cell-based cancer immunotherapy. Nat Nanotechnol. 2011; 6:675–82. [PubMed: 21909083]
69. Guo D, Wu C, Jiang H, et al. Synergistic cytotoxic effect of different sized ZnO nanoparticles and daunorubicin against leukemia cancer cells under UV irradiation. J Photochem Photobiol B. 2008; 93:119–26. [PubMed: 18774727]
70. Li J, Guo D, Wang X, et al. The Photodynamic Effect of Different Size ZnO Nanoparticles on Cancer Cell Proliferation In Vitro. Nanoscale Res Lett. 2010; 5:1063–71. [PubMed: 20671778]

71. Brown SB, Brown EA, Walker I. The present and future role of photodynamic therapy in cancer treatment. Lancet Oncol. 2004; 5:497–508. [PubMed: 15288239]
72. Wilson BC, Patterson MS. The physics, biophysics and technology of photodynamic therapy. Phys Med Biol. 2008; 53:R61–109. [PubMed: 18401068]
73. Zhang H, Chen B, Jiang H, et al. A strategy for ZnO nanorod mediated multi-mode cancer treatment. Biomaterials. 2011; 32:1906–14. [PubMed: 21145104]
74. McCormick F. Cancer gene therapy: fringe or cutting edge? Nat Rev Cancer. 2001; 1:130–41. [PubMed: 11905804]
75. Nie L, Gao L, Feng P, et al. Three-dimensional functionalized tetrapod-like ZnO nanostructures for plasmid DNA delivery. Small. 2006; 2:621–5. [PubMed: 17193097]
76. Nie L, Gao L, Yan X, Wang T. Functionalized tetrapod-like ZnO nanostructures for plasmid DNA purification, polymerase chain reaction and delivery. Nanotechnology. 2007; 18:015101.
77. Zhang P, Liu W. ZnO QD@PMAA-co-PDMAEMA nonviral vector for plasmid DNA delivery and bioimaging. Biomaterials. 2010; 31:3087–94. [PubMed: 20096454]
78. Zhao Z, Lei W, Zhang X, Wang B, Jiang H. ZnO-Based Amperometric Enzyme Biosensors. Sensors (Basel). 2010; 10:1216–31. [PubMed: 22205864]
79. Wang JX, Sun XW, Wei A, et al. Zinc oxide nanocomb biosensor for glucose detection. Appl Phys Lett. 2006; 88:233106.
80. Kumar SA, Chen SM. Nanostructured zinc oxide particles in chemically modified electrodes for biosensor applications. Anal Lett. 2008; 41:141–58.
81. Willander M, Al-Hilli S. ZnO nanorods as an intracellular sensor for pH measurements. Methods Mol Biol. 2009; 544:187–200. [PubMed: 19488701]
82. Pachauri V, Vlandas A, Kern K, Balasubramanian K. Site-specific self-assembled liquid-gated ZnO nanowire transistors for sensing applications. Small. 2010; 6:589–94. [PubMed: 19842112]
83. Anish, Kumar M.; Jung, S.; Ji, T. Protein biosensors based on polymer nanowires, carbon nanotubes and zinc oxide nanorods. Sensors (Basel). 2011; 11:5087–111. [PubMed: 22163892]
84. Zang JF, Li CM, Cui XQ, et al. Tailoring zinc oxide nanowires for high performance amperometric glucose sensor. Electroanalysis. 2007; 19:1008–14.
85. Weber J, Jeedigunta S, Kumar A. Fabrication and Characterization of ZnO Nanowire Arrays with an Investigation into Electrochemical Sensing Capabilities. J Nanomater. 2008:638523.
86. Wei A, Sun XW, Wang JX, et al. Enzymatic glucose biosensor based on ZnO nanorod array grown by hydrothermal decomposition. Appl Phys Lett. 2006; 89:123902.
87. Umar A, Rahman MM, Kim SH, Hahn YB. ZnO nanonails: synthesis and their application as glucose biosensor. J Nanosci Nanotechnol. 2008; 8:3216–21. [PubMed: 18681071]
88. Dai ZH, Shao GJ, Hong JM, Bao JC, Shen J. Immobilization and direct electrochemistry of glucose oxidase on a tetragonal pyramid-shaped porous ZnO nanostructure for a glucose biosensor. Biosens Bioelectron. 2009; 24:1286–91. [PubMed: 18774704]
89. Wei Y, Li Y, Liu X, et al. ZnO nanorods/Au hybrid nanocomposites for glucose biosensor. Biosens Bioelectron. 2010; 26:275–8. [PubMed: 20598519]
90. Zhao ZW, Chen XJ, Tay BK, et al. A novel amperometric biosensor based on ZnO : Co nanoclusters for biosensing glucose. Biosens Bioelectron. 2007; 23:135–9. [PubMed: 17478087]
91. Liu JP, Guo CX, Li CM, et al. Carbon-decorated ZnO nanowire array: A novel platform for direct electrochemistry of enzymes and biosensing applications. Electrochem Commun. 2009; 11:202–5.
92. Sung YM, Noh K, Kwak WC, Kim TG. Enhanced glucose detection using enzyme-immobilized ZnO/ZnS core/sheath nanowires. Sensor Actuat B-Chem. 2012; 161:453–9.
93. Hu FX, Chen SH, Wang CY, et al. ZnO nanoparticle and multiwalled carbon nanotubes for glucose oxidase direct electron transfer and electrocatalytic activity investigation. J Mol Catal B-Enzym. 2011; 72:298–304.
94. Kim KE, Kim TG, Sung YM. Enzyme-conjugated ZnO nanocrystals for collisional quenching-based glucose sensing. Crystengcomm. 2012; 14:2859–65.
95. Wang G, Xu JJ, Ye LH, Zhu JJ, Chen HY. Highly sensitive sensors based on the immobilization of tyrosinase in chitosan. Bioelectrochemistry. 2002; 57:33–8. [PubMed: 12049754]

96. Dempsey E, Diamond D, Collier A. Development of a biosensor for endocrine disrupting compounds based on tyrosinase entrapped within a poly(thionine) film. Biosens Bioelectron. 2004; 20:367–77. [PubMed: 15308243]

97. de Albuquerque YDT, Ferreira LF. Amperometric biosensing of carbamate and organophosphate pesticides utilizing screen-printed tyrosinase-modified electrodes. Analytica Chimica Acta. 2007; 596:210–21. [PubMed: 17631099]

98. Liu ZM, Liu YL, Yang HF, et al. A mediator-free tyrosinase biosensor based on ZnO sol-gel matrix. Electroanalysis. 2005; 17:1065–70.

99. Li YF, Liu ZM, Liu YL, et al. A mediator-free phenol biosensor based on immobilizing tyrosinase to ZnO nanoparticles. Anal Biochem. 2006; 349:33–40. [PubMed: 16384546]

100. Chen LY, Gu BX, Zhu GP, et al. Electron transfer properties and electrocatalytic behavior of tyrosinase on ZnO nanorod. J Electroanal Chem. 2008; 617:7–13.

101. Zhao J, Zhi J, Zhou Y, Yan W. A tyrosinase biosensor based on ZnO nanorod clusters/ nanocrystalline diamond electrodes for biosensing of phenolic compounds. Anal Sci. 2009; 25:1083–8. [PubMed: 19745534]

102. Gu BX, Xu CX, Zhu GP, et al. Tyrosinase Immobilization on ZnO Nanorods for Phenol Detection. J Phys Chem B. 2009; 113:377–81. [PubMed: 19067557]

103. Zhao JW, Wu DH, Zhi JF. A novel tyrosinase biosensor based on biofunctional ZnO nanorod microarrays on the nanocrystalline diamond electrode for detection of phenolic compounds. Bioelectrochemistry. 2009; 75:44–9. [PubMed: 19230793]

104. Lee JM, Xu GR, Kim BK, Choi HN, Lee WY. Amperometric Tyrosinase Biosensor Based on Carbon Nanotube-Doped Sol-Gel-Derived Zinc Oxide-Nafion Composite Films. Electroanalysis. 2011; 23:962–70.

105. Zhang YW, Zhang Y, Wang H, et al. An enzyme immobilization platform for biosensor designs of direct electrochemistry using flower-like ZnO crystals and nano-sized gold particles. J Electroanal Chem. 2009; 627:9–14.

106. Liu YL, Yang YH, Yang HF, et al. Nanosized flower-like ZnO synthesized by a simple hydrothermal method and applied as matrix for horseradish peroxidase immobilization for electro-biosensing. J Inorg Biochem. 2005; 99:2046–53. [PubMed: 16095710]

107. Cao X, Ning W, Li LD, Guo L. Synthesis and characterization of waxberry-like microstructures ZnO for biosensors. Sensor Actuat B-Chem. 2008; 129:268–73.

108. Gu BX, Xu CX, Zhu GP, et al. Layer by layer immobilized horseradish peroxidase on zinc oxide nanorods for biosensing. J Phys Chem B. 2009; 113:6553–7. [PubMed: 19358542]

109. Sullivan DR. Screening for cardiovascular disease with cholesterol. Clin Chim Acta. 2002; 315:49–60. [PubMed: 11728410]

110. Wilkinson IB, Cockcroft JR. Cholesterol, endothelial function and cardiovascular disease. Curr Opin Lipidol. 1998; 9:237–42. [PubMed: 9645507]

111. Umar A, Rahman MM, Vaseem M, Hahn YB. Ultra-sensitive cholesterol biosensor based on low-temperature grown ZnO nanoparticles. Electrochem Commun. 2009; 11:118–21.

112. Singh SP, Arya SK, Pandey P, et al. Cholesterol biosensor based on rf sputtered zinc oxide nanoporous thin film. Appl Phys Lett. 2007; 91:063901.

113. Umar A, Rahman MM, Al-Hajry A, Hahn YB. Highly-sensitive cholesterol biosensor based on well-crystallized flower-shaped ZnO nanostructures. Talanta. 2009; 78:284–9. [PubMed: 19174239]

114. Ahmad M, Pan CF, Gan L, Nawaz Z, Zhu J. Highly Sensitive Amperometric Cholesterol Biosensor Based on Pt-Incorporated Fullerene-like ZnO Nanospheres. J Phys Chem C. 2010; 114:243–50.

115. Wang CY, Tan XR, Chen SH, et al. Highly-sensitive cholesterol biosensor based on platinum-gold hybrid functionalized ZnO nanorods. Talanta. 2012; 94:263–70. [PubMed: 22608446]

116. Israr MQ, Sadaf JR, Asif MH, et al. Potentiometric cholesterol biosensor based on ZnO nanorods chemically grown on Ag wire. Thin Solid Films. 2010; 519:1106–9.

117. Israr MQ, Sadaf JR, Nur O, et al. Chemically fashioned ZnO nanowalls and their potential application for potentiometric cholesterol biosensor. Appl Phys Lett. 2011; 98:253705.

118. Rajesh, Bisht V, Takashima W, Kaneto K. An amperometric urea biosensor based on covalent immobilization of urease onto an electrochemically prepared copolymer poly (N-3-aminopropyl pyrrole-co-pyrrole) film. Biomaterials. 2005; 26:3683–90. [PubMed: 15744952]
119. Solanki PR, Kaushik A, Ansari AA, Sumana G, Malhotra BD. Zinc oxide-chitosan nanobiocomposite for urea sensor. Appl Phys Lett. 2008; 93:163903.
120. Ali A, Ansari AA, Kaushik A, et al. Nanostructured zinc oxide film for urea sensor. Mater Lett. 2009; 63:2473–5.
121. Palomera N, Balaguera M, Arya SK, et al. Zinc oxide nanorods modified indium tin oxide surface for amperometric urea biosensor. J Nanosci Nanotechnol. 2011; 11:6683–9. [PubMed: 22103068]
122. Ali SMU, Ibupoto ZH, Salman S, et al. Selective determination of urea using urease immobilized on ZnO nanowires. Sensor Actuat B-Chem. 2011; 160:637–43.
123. Rout CS, Raju AR, Govindaraj A, Rao CN. Ethanol and hydrogen sensors based on ZnO nanoparticles and nanowires. J Nanosci Nanotechnol. 2007; 7:1923–9. [PubMed: 17654966]
124. Lei Y, Liu X, Yan X, et al. Multicenter uric acid biosensor based on tetrapod-shaped ZnO nanostructures. J Nanosci Nanotechnol. 2012; 12:513–8. [PubMed: 22524012]
125. Usman, Ali SM.; Ibupoto, ZH.; Kashif, M.; Hashim, U.; Willander, M. A Potentiometric Indirect Uric Acid Sensor Based on ZnO Nanoflakes and Immobilized Uricase. Sensors (Basel). 2012; 12:2787–97. [PubMed: 22736977]
126. Ibupoto ZH, Ali Shah SM, Khun K, Willander M. Electrochemical l-Lactic Acid Sensor Based on Immobilized ZnO Nanorods with Lactate Oxidase. Sensors (Basel). 2012; 12:2456–66. [PubMed: 22736960]
127. Leiterer C, Seise B, Slowik I, et al. DNA hybridization assay at individual, biofunctionalized zinc oxide nanowires. J Biophotonics. 2012 Epub ahead of print.
128. Yumak T, Kuralay F, Muti M, et al. Preparation and characterization of zinc oxide nanoparticles and their sensor applications for electrochemical monitoring of nucleic acid hybridization. Colloids Surf B Biointerfaces. 2011; 86:397–403. [PubMed: 21600741]
129. Tawa K, Umetsu M, Hattori T, Kumagai I. Zinc oxide-coated plasmonic chip modified with a bispecific antibody for sensitive detection of a fluorescent labeled-antigen. Anal Chem. 2011; 83:5944–8. [PubMed: 21692512]
130. Chang CC, Chiu NF, Lin DS, et al. High-sensitivity detection of carbohydrate antigen 15-3 using a gold/zinc oxide thin film surface plasmon resonance-based biosensor. Anal Chem. 2010; 82:1207–12. [PubMed: 20102177]
131. Whitesides GM. Nanoscience, nanotechnology, and chemistry. Small. 2005; 1:172–9. [PubMed: 17193427]
132. Service RF. Molecular electronics. Nanodevices make fresh strides toward reality. Science. 2003; 302:1310. [PubMed: 14631005]
133. Rasmussen JW, Martinez E, Louka P, Wingett DG. Zinc oxide nanoparticles for selective destruction of tumor cells and potential for drug delivery applications. Expert Opin Drug Deliv. 2010; 7:1063–77. [PubMed: 20716019]
134. Muller KH, Kulkarni J, Motskin M, et al. pH-dependent toxicity of high aspect ratio ZnO nanowires in macrophages due to intracellular dissolution. ACS Nano. 2010; 4:6767–79. [PubMed: 20949917]
135. George S, Pokhrel S, Xia T, et al. Use of a rapid cytotoxicity screening approach to engineer a safer zinc oxide nanoparticle through iron doping. ACS Nano. 2010; 4:15–29. [PubMed: 20043640]
136. Nair S, Sasidharan A, Divya Rani VV, et al. Role of size scale of ZnO nanoparticles and microparticles on toxicity toward bacteria and osteoblast cancer cells. J Mater Sci Mater Med. 2009; 20(Suppl 1):S235–411. [PubMed: 18716714]
137. Wang ZL. Nanostructures of zinc oxide. Mater Today. 2004; 7:26–33.

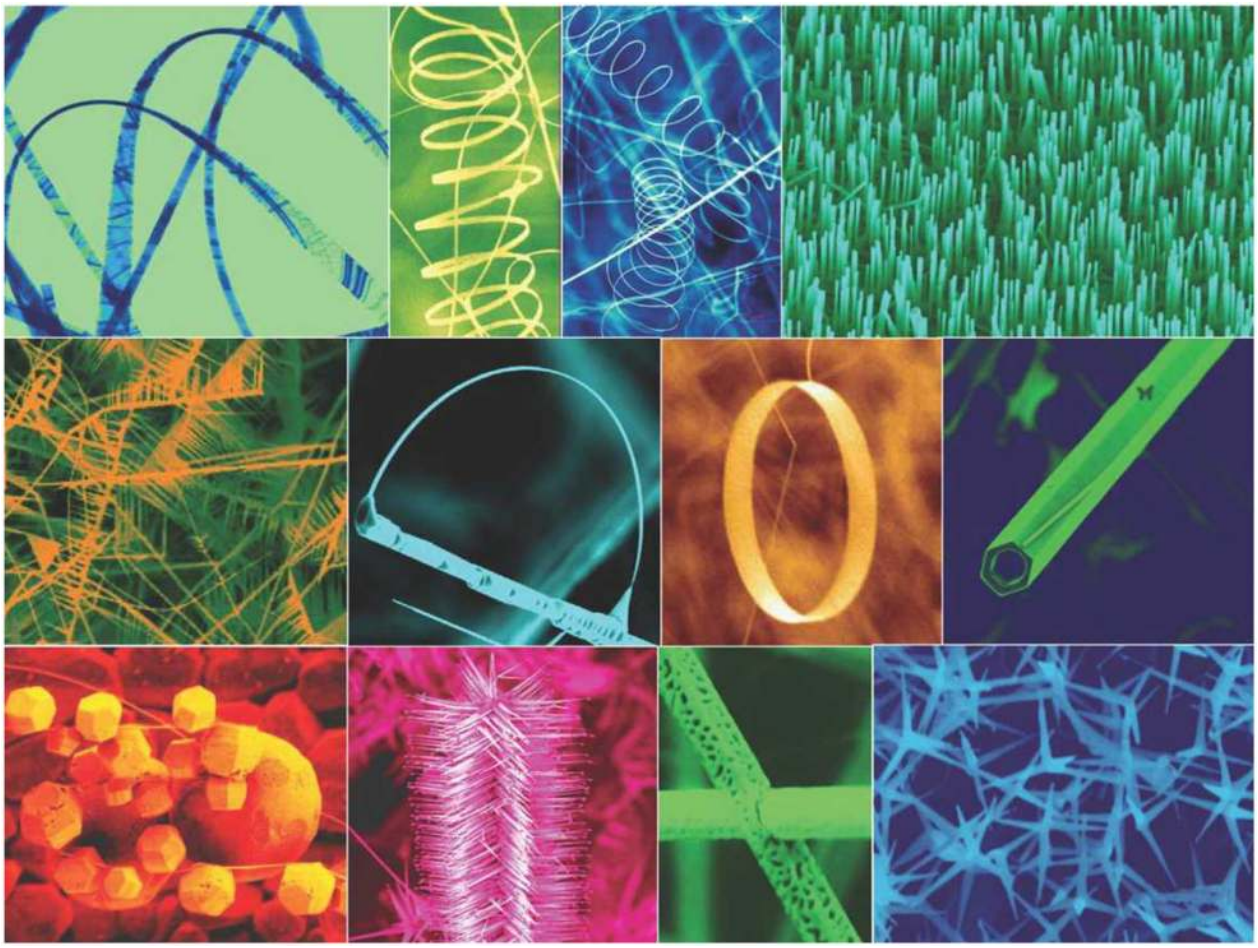

Fig. (1).
ZnO can be synthesized to display a wide variety of nanostructures. Adapted from [137].

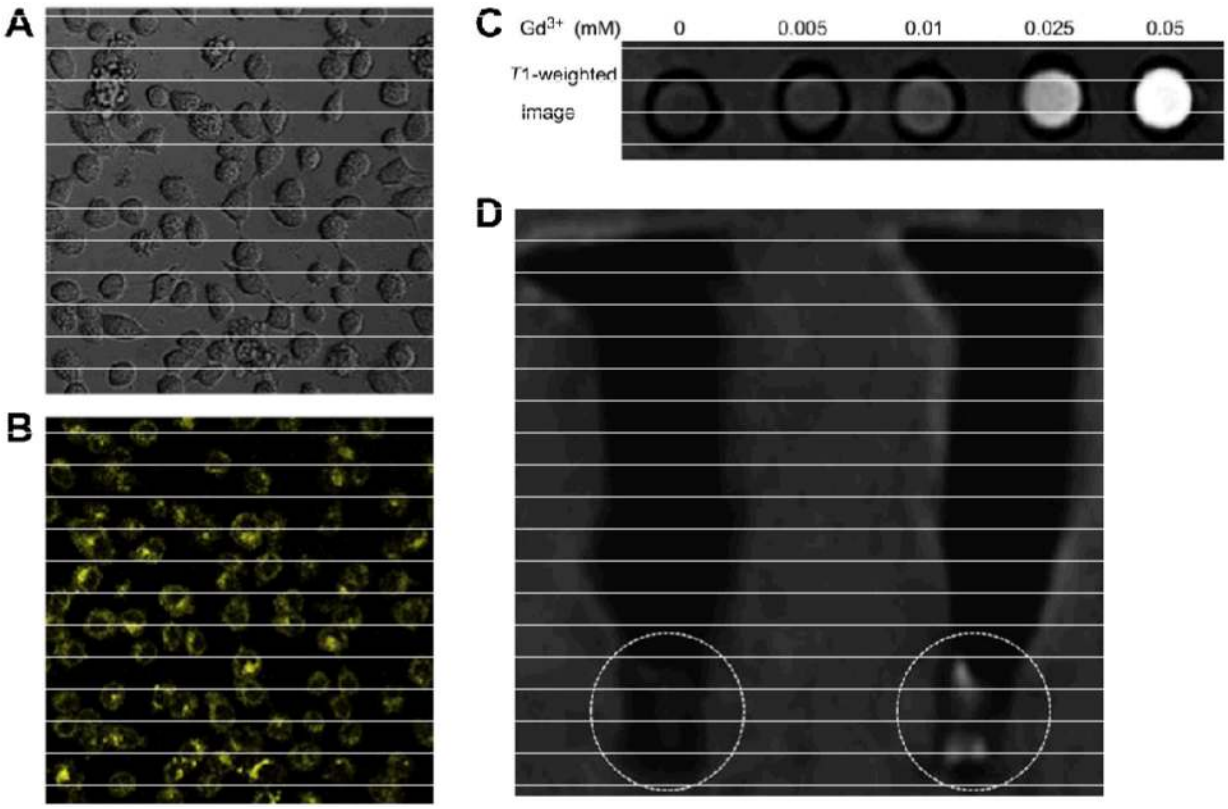

Fig. (2).

MRI and optical imaging with Gd-doped ZnO QDs. White field (**A**) and fluorescence (**B**) images of HeLa cells after incubation with Gd-doped ZnO QDs. **C.** A T_1-weighted MRI image of aqueous solutions of Gd-doped ZnO QDs with various Gd^{3+} concentrations, obtained with a 1.5 T clinical MRI system. **D.** A T_1-weighted image of HeLa cells pellet without (left) and with Gd-doped ZnO QDs (right). Adapted from [42].

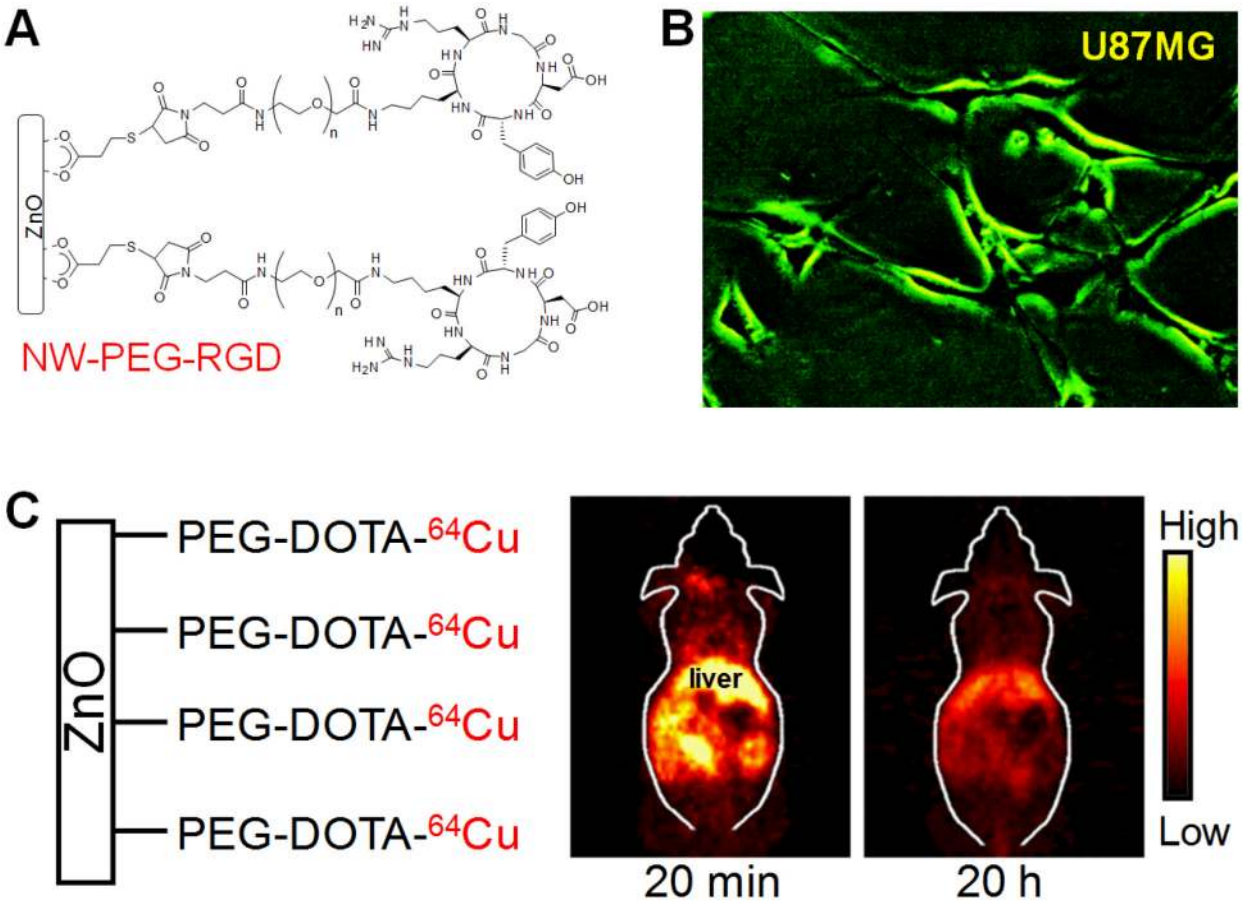

Fig. (3).

Targeted optical imaging with green fluorescent ZnO nanowires (NWs). **A.** A schematic structure of RGD peptide conjugated ZnO NWs. PEG denotes polyethylene glycol. **B.** Fluorescence imaging of integrin $\alpha_v\beta_3$ on U87MG human glioblastoma cells with NW-PEG-RGD. Magnification: 200×. **C.** Representatives positron emission tomography images of ^{64}Cu-labeled non-targeted ZnO NWs at 20 min and 20 h postinjection into female Balb/c mice. Adapted from [44].

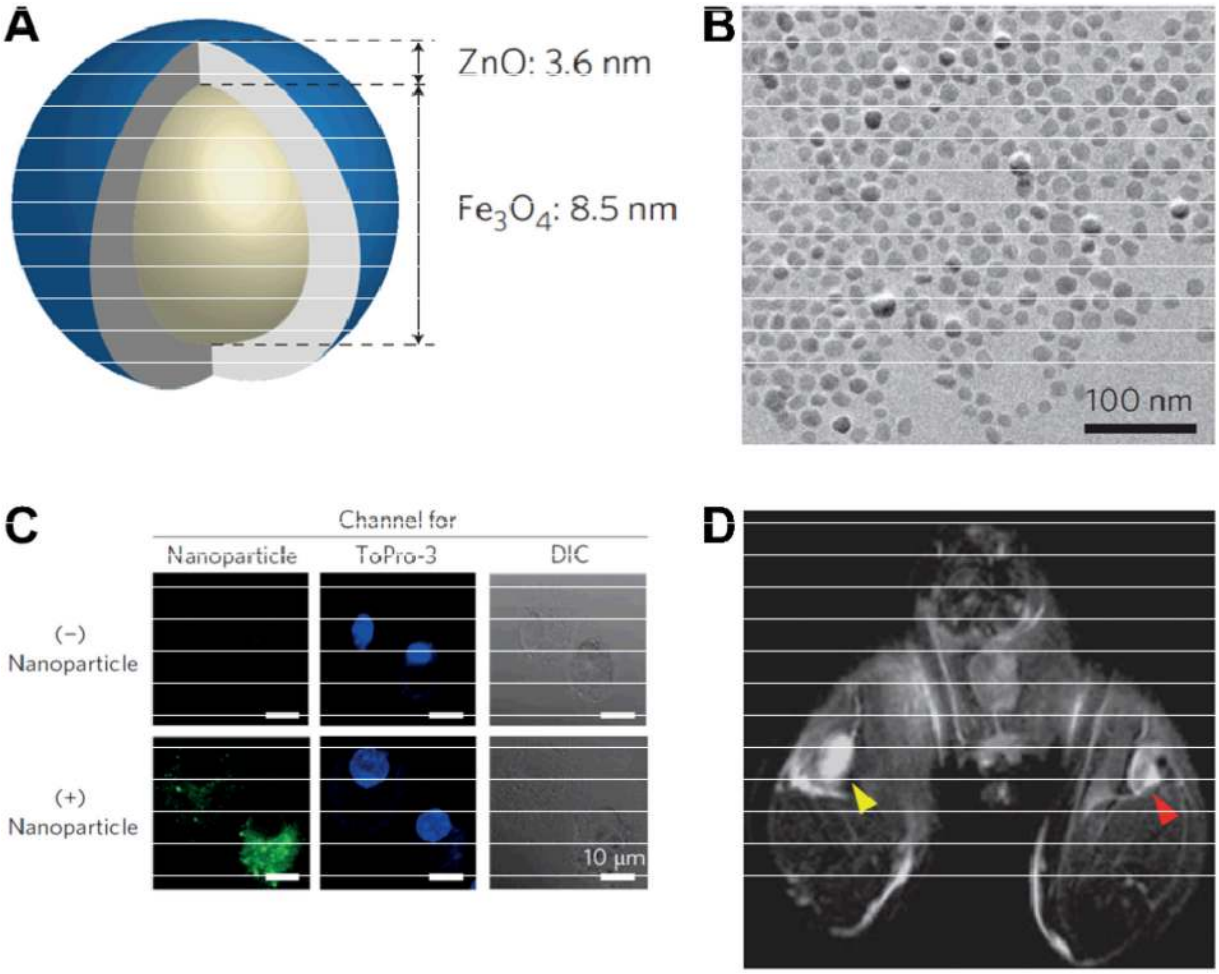

Fig. (4).

A. A diagram of the core-shell Fe_3O_4-ZnO nanoparticle. **B.** A transmission electron microscopy image of the core-shell Fe_3O_4-ZnO nanoparticles. **C.** Fluorescence images of dendritic cells (DCs) without (top) or with (bottom) the nanoparticles. The fluorescence signal is shown in green and the nuclei (in blue) were stained with ToPro-3. DIC: differential interference contrast. **D.** An in vivo MRI image of draining lymph nodes of a mouse injected with DCs labeled with Fe_3O_4-ZnO (red arrowhead) or ZnO nanoparticles (yellow arrowhead) into the ipsilateral footpads. Adapted from [68].

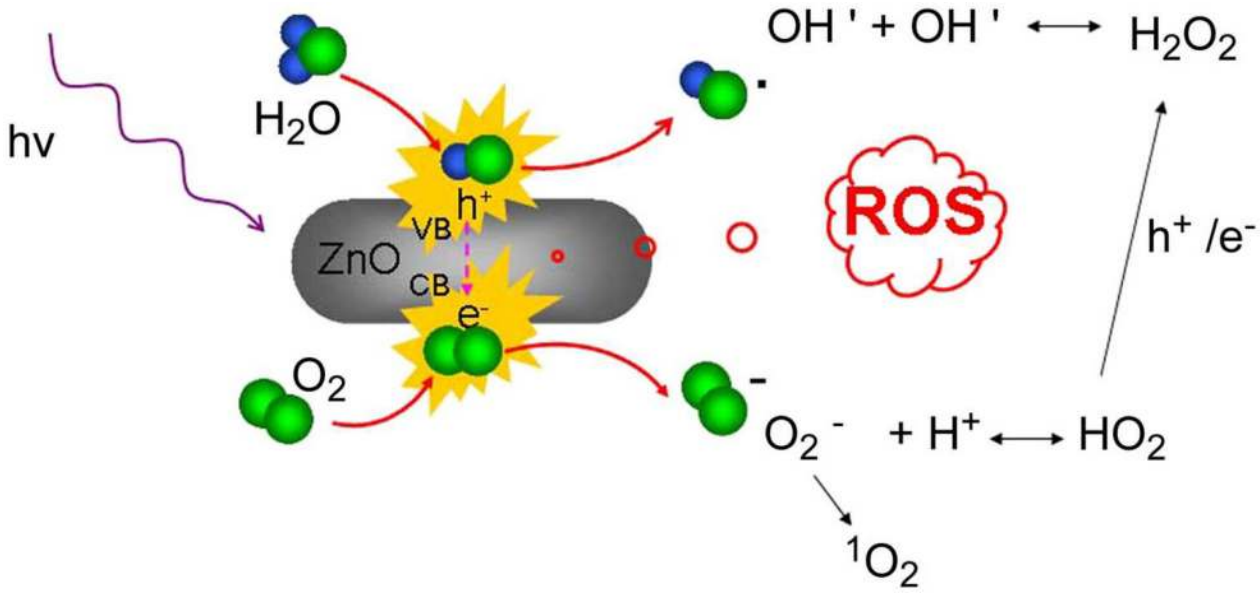

Fig. (5).
Possible mechanism of reactive oxygen species (ROS) production by ZnO nanorods under UV irradiation. Adapted from [73].

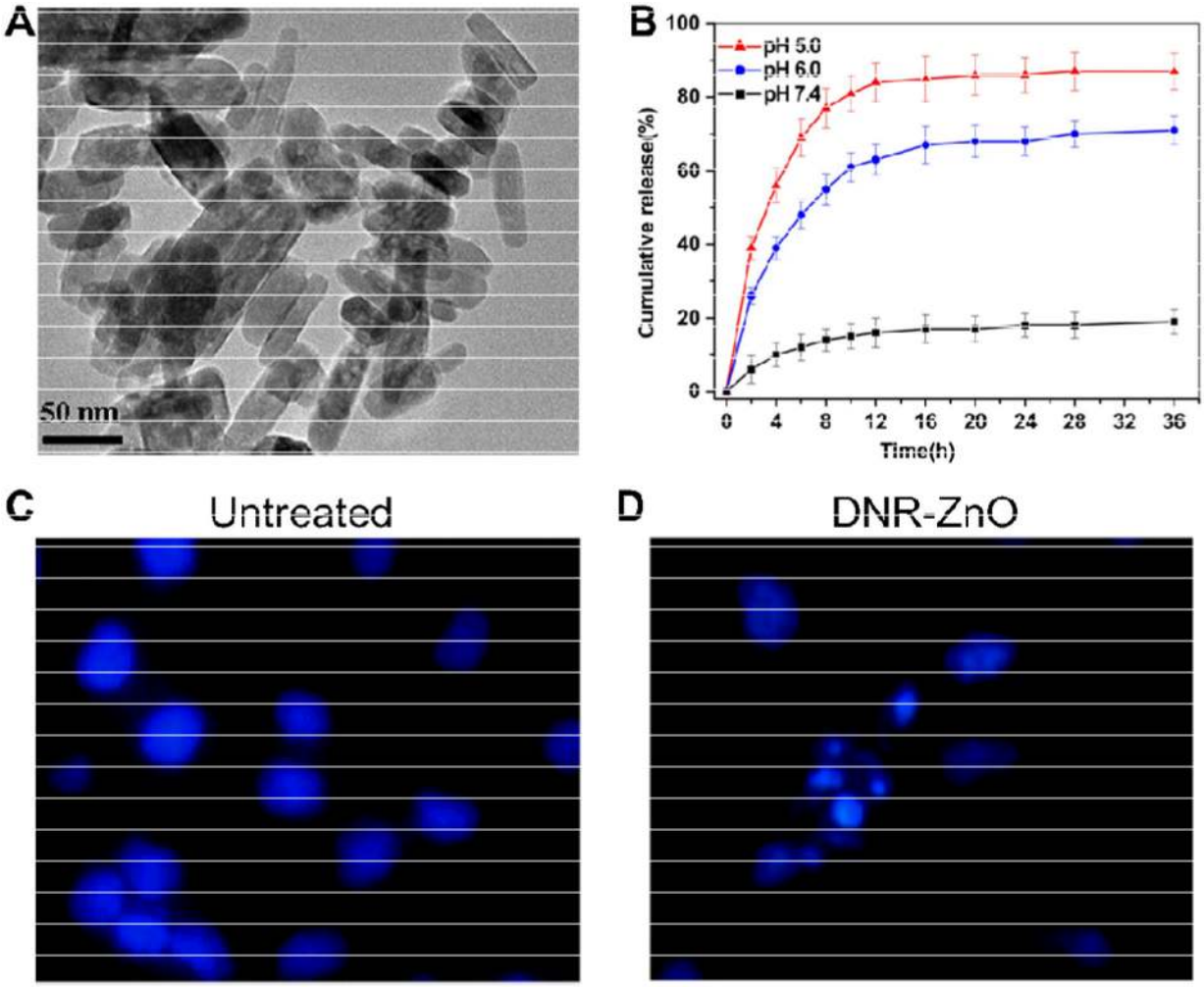

Fig. (6).

A. A transmission electron microscopy image of ZnO nanorods. **B.** In vitro daunorubicin (DNR) release profiles at pH 7.4, 6.0, and 5.0. Nuclear morphologic changes of untreated SMCC-7721 cells (**C**) or cells treated with DNR-ZnO nanocomposites upon UV irradiation (which showed features of apoptosis; **D**). Magnification: 400×. Adapted from [73].

Table 1

A selected list of ZnO-based biosensors which use immobilized enzymes.

Analyte	ZnO Nanostructure	Immobilization Mode	Detection Limit (μM)	References
	Nanocombs	Physical adsorption	20	[79]
	Nanowires	Physical adsorption	0.7	[84]
	Nanowire arrays	Physical adsorption	100	[85]
	Nanorods	Electrostatic	10	[86]
	Nanonails	Electrostatic	5	[87]
	Tetragonal pyramid-shaped porous ZnO nanostructures	Physical adsorption	10	[88]
Glucose	Nanorods	Crosslinking	0.01	[89]
	Nanoclusters	Crosslinking	20	[90]
	Carbon decorated Nanowires	Physical adsorption	1	[91]
	Nanoparticles	Physical adsorption	2.2	[93]
	Nanocrystals	Covalent bonding	330	[94]
	Nanowires	Covalent bonding	140	[92]
	ZnO sol-gel matrix	Electrostatic	0.08	[98]
	Nanoparticles	Electrostatic	0.05	[99]
	Nanorods	Electrostatic	15.6	[100]
Phenol	Nanorod cluster	Electrostatic	0.5	[101]
	Nanorods	Electrostatic	0.63	[102]
	Nanorod microarray	Covalent bonding	0.25	[103]
	Nanofilm	Encapsulation	0.047	[104]
	Nanoflower	Entrapment	2.0	[106]
H_2O_2	Nanorods	Chemical adsorption	0.12	[107]
	Nanorods on gold wire	Physical adsorption	5	[108]
	Nanoporous thin film	Physical adsorption	/	[112]
	Flower shaped nanostructure	Physical adsorption	0.012	[113]
Cholesterol	Nanospheres	Physical adsorption	0.5	[114]
	Nanorods	Electrostatic	0.03	[115]
	Nanorods	Electrostatic	1	[116]
	Nanorods	Electrostatic	1	[117]
	Nanobiocomposite film	Physical adsorption	3mg/dl	[119]
Urea	Nanofilm	Physical adsorption	13.5 mg/dl	[120]
	Nanorods	Electrostatic	0.4	[121]
	Nanowires	Physical adsorption	/	[122]